

Sulphidation of cobalt at high temperatures

S. MROWEC, M. DANIELEWSKI, A. WÓJTOWICZ

University of Mining and Metallurgy, Department of Solid State Chemistry,

al. Mickiewicza 30, 30-059 Cracow, Poland

E-mail: mdaniel@scientist.com

The kinetics and mechanism of cobalt sulphidation have been studied as a function of temperature (773–1023 K) and sulphur partial pressure ($1-10^4$ Pa) by means of thermogravimetric, SEM and X-ray techniques, and also using inert-marker and ratio-tracer methods. It has been shown that the sulphidation process is diffusion controlled, the rate-determining step being the outward *volume* diffusion of cations. According to the phase diagram of the Co–S system, the sulphide scale on cobalt is heterogeneous. At sulphur pressures higher than the dissociation pressure of the CoS_2 phase, the sulphidation rate is pressure independent, and at lower pressures it increases with rising pressure, in agreement with theoretical predictions. The apparent activation energy of sulphidation is considerably higher for multilayer than for double-layer scale formation, because the main part of multilayer scale is growing at the dissociation pressure of the CoS_2 phase, which increases with increasing temperature. Over the whole temperature and pressure range studied, the rate of cobalt sulphidation is more than three orders of magnitude higher than the oxidation rate of this metal. Rapid degradation of cobalt in a sulphur atmosphere results mainly from a very high defect concentration in Co_{1-y}S and Co_9S_8 sulphides, participating in comparable amounts in the scale formation on this metal at $T > 900$ K. The only sulphide of cobalt in which the defect concentration may be very low is CoS_2 , the growth rate of this sulphide layer being more than two orders of magnitude lower than that of other cobalt sulphides. © 1998 Chapman & Hall

1. Introduction

In many branches of modern technology, metallic materials are exposed to sulphur-containing atmospheres at high temperatures [1]. Under these conditions, all conventional oxidation-resistant alloys undergo very rapid, often catastrophic degradation [1–4]. This is the reason why sulphidation of metals and alloys has received much attention for many years. In spite of this, however, the mechanism of sulphide corrosion is still less known than that of metal oxidation [1, 3, 4]. Such a situation results mainly from much greater experimental difficulties in studying the high-temperature reactions in sulphur-containing atmospheres and from the fact that transition metal sulphides are much more numerous than the corresponding oxides [3, 4]. For instance, in the cobalt–oxygen system there is only one thermodynamically stable oxide at high temperatures, while in the cobalt–sulphur system at least five sulphides are stable at elevated temperatures. The defect and transport properties of these sulphides remain unexplained, except those of Co_{1-y}S . These are the main reasons why the mechanism of cobalt sulphidation is still not fully understood. On the other hand, detailed knowledge of this problem is needed for better understanding of high-temperature corrosion of cobalt-base superalloys in sulphur-containing atmospheres [1, 5].

The aim of the present work was to obtain further information on the cobalt sulphidation in systematic studies of the kinetics and mechanisms of this process as a function of temperature and sulphur activity.

2. General remarks

Sulphidation of cobalt has been studied by Devin [6], Coutsouradis and Devin [7], Whittle *et al.* [8] and also by Mrowec and co-workers [9, 10] in $\text{H}_2/\text{H}_2\text{S}$ gas mixtures and in pure sulphur vapour at temperatures from 770–1273 K. It has been found that independently of temperature and atmosphere used, cobalt sulphidation follows parabolic kinetics, being thus diffusion controlled. Marker experiments, in turn, have shown that the sulphide scale on cobalt grows mainly by the outward diffusion of cations [7], which implies that the latter processes are the rate-determining step of cobalt sulphidation under the discussed conditions.

The parabolic rate constants for the sulphidation of cobalt as a function of temperature are summarized in Fig. 1. The effect of sulphur pressure on the sulphidation rate of cobalt has been studied only by Devin [6] in a very narrow pressure range, 1.3×10^4 – 5.2×10^4 Pa. From Fig. 1 it follows that the activation energy of the cobalt sulphidation, determined by different authors, varies considerably between 78 and 311 kJ mol^{-1} ,

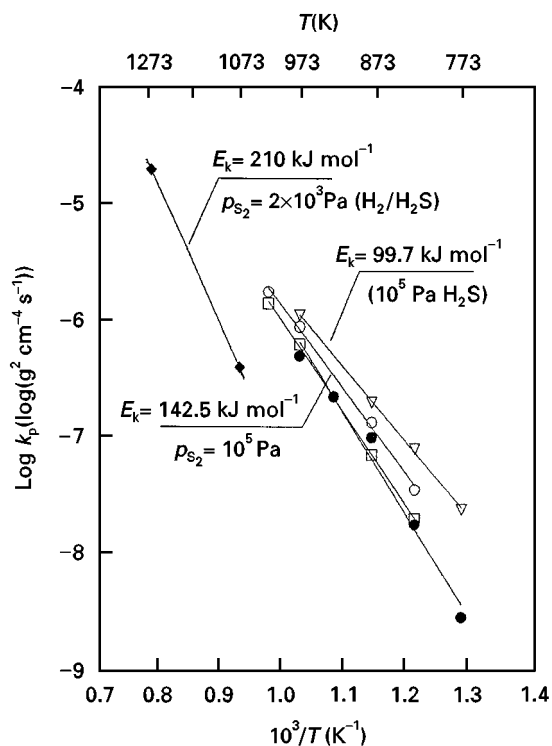


Figure 1 The parabolic rate constants for the sulphidation of cobalt as a function of temperature [6–10]. (□) [9], (●) [6], (▽) [7], (◆) [8], (○) [10].

depending on atmosphere and temperature range used. It should be noted that all kinetic data, except that of Whittle *et al.* [8], has been obtained under conditions corresponding to the thermodynamic stability of the highest cobalt sulphide, i.e. the CoS_2 phase. Thus, the scale was heterogeneous and built of several phases, as can be inferred from the part of the Co–S phase diagram shown in Fig. 2, in which the conditions of previous and present sulphidation experiments are also marked.

This phase diagram was constructed using Rosenquist's [11, 12] (solid line) and Rau's [13] (dotted line) data. As can be seen, there is fairly good agreement between both results, except those concerning the $\text{Co}_{1-y}\text{S}/\text{CoS}_2$ phase boundary, where the more recent and accurate Rau's data suggest a wider homogeneity range for the Co_{1-y}S phase. Very high deviations from stoichiometry of this sulphide result from cation sublattice disorder, in which the concentration of cation vacancies may reach the enormous values of 18 at % ($\text{Co}_{0.82}\text{S}$) [13]. The defect structures of the remaining cobalt sulphides are unknown, but from the thermodynamic studies of Chen and Chang [14] it can be inferred that Co_9S_8 and Co_3S_4 sulphides are also highly disordered. The CoS_2 phase, on the other hand, is believed to exist in a very narrow homogeneity range.

Based on the phase diagram presented in Fig. 2, one can predict the phase composition of the scale formed under given thermodynamic conditions. However, available literature data are not in agreement with such predictions. For instance, Devin and Coutouradis [7] Mrowec and co-workers [9, 10], and also Bartkiewicz and Stokłosa [15] sulphidized cobalt under conditions of thermodynamic stability of the CoS_2 phase. When the diffusivities in the scale-form-

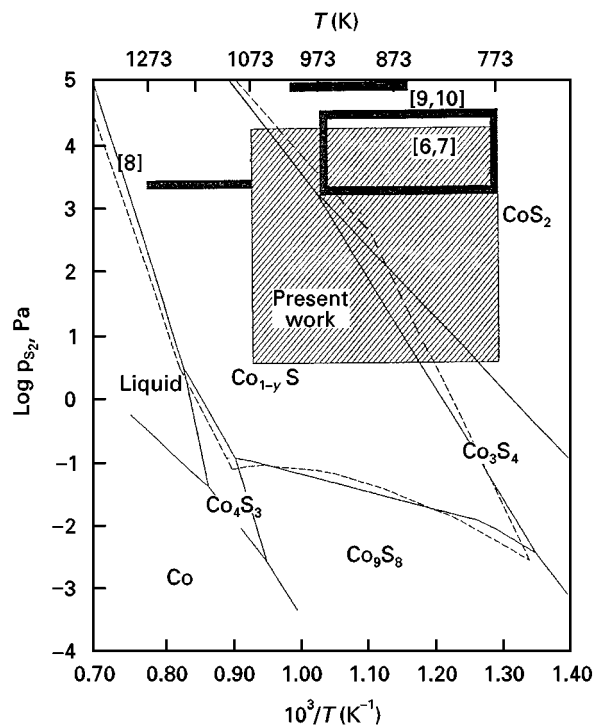


Figure 2 Part of the Co–S phase diagram [11–13]. The dimensions of the bars and boxes show the temperature and pressure range studied in this work.

ing sulphides are of the same order of magnitude, and the mass transport at interphases is not a rate-limiting step, the scale should then contain all the sulphides occurring at a given temperature in the Co–S system (Fig. 2). However, Devin [6] found two-phase scales built of Co_9S_8 and Co_3S_4 sulphides, while Mrowec and Werber [9] reported a homogeneous scale composed of Co_{1-y}S sulphide only. Bartkiewicz and Stokłosa [15], in turn, found three phases in their scales (Co_9S_8 , Co_{1-y}S and Co_3S_4) but none of the authors could detect the highest CoS_2 phase on the surface of the sulphide scales formed on cobalt under the discussed conditions.

Thus, to obtain greater insight into the mechanism of cobalt sulphidation, our experimental conditions were chosen so that the sulphidation process could be followed as a function of temperature and sulphur pressure, both below and above the thermodynamic stability of the CoS_2 and Co_3S_4 phases. Consequently, in the first case ($p_{\text{S}_2} < p_{\text{CoS}_2}^d$ and $T > 900$ K) double-layer, two-phase scales built of Co_9S_8 and Co_{1-y}S sulphides were expected (see Fig. 2) and in the second case ($p_{\text{S}_2} > p_{\text{CoS}_2}^d$ and $T > 900$ K), triple-layer scales with the CoS_2 uppermost layer were anticipated to form ($p_{\text{CoS}_2}^d$ denotes the dissociation pressure of CoS_2). However, at temperatures lower than 900 K, the Co_3S_4 phase can also be formed (Fig. 2). Thus, at $T < 900$ K and $p_{\text{S}_2} > p_{\text{CoS}_2}^d$, a four-layer scale can form, constituting the following heterogeneous system: $\text{Co}/\text{Co}_9\text{S}_8/\text{Co}_{1-y}\text{S}/\text{Co}_3\text{S}_4/\text{CoS}_2/\text{S}_2$. On gradually lowering the sulphur pressure, one can expect the formation of a triple-layer ($\text{Co}_9\text{S}_8/\text{Co}_{1-y}\text{S}/\text{Co}_3\text{S}_4$) scale and finally of a double-layer ($\text{Co}_9\text{S}_8/\text{Co}_{1-y}\text{S}$) scale, as in the case of sulphidation at temperatures higher than 900 K.

3. Experimental procedure

Spectrally pure cobalt, produced by Johnson-Mathey Chemical Ltd, with an impurity content not exceeding 5 p.p.m. was used in this study. Plates of this metal were abraded with a diamond disc to a thickness of about 1 mm and subsequently ground with emery papers down to 800 grade and polished with diamond paste. The specimens with mirror-like surfaces were washed ultrasonically in ethyl alcohol and acetone and stored in acetone until required for the sulphidation experiments. The surface area of those specimens with a thickness of 0.06 cm was about 4 cm². The sulphur used contained less than 0.02 wt% impurities. To remove dissolved and absorbed gases, sulphur was melted many times under a high vacuum before each series of sulphidation experiments.

Kinetic measurements have been carried out thermogravimetrically as a function of temperature (773–1023 K) and sulphur vapour pressure (1–10⁴ Pa) in He–S₂ mixtures thus enabling the sulphidation process to be followed in a wide pressure range under dynamic conditions.

The sulphidation rate was measured in the microthermobalance shown schematically in Fig. 3. The main difference between this device and other equipment currently used in studying the sulphidation kinetics in sulphur vapour consists of mixing these vapours with a carrier gas (helium), the flow rate of which together with the temperature of the liquid sulphur bath determine the partial pressure of the sulphur vapour in the gas mixture at a total pressure of 1 atm. The discussed assembly comprises three main parts: a container with the liquid sulphur being its vapour sources (3), a thermogravimetric system

with the spiral balance (2) and a reaction chamber (4), as well as the helium dosage system (5, 6) and the balance space.

A spiral balance is made of Ni-Span-C-alloy, the elastic properties and thermal coefficient of which are constant in the 10–65°C temperature range, and therefore it does not require any thermostating. The spiral, consisting of 36 coils (diameter 12 mm) conserves its linear elongation coefficient up to 1 g and within these limits enables reproducible measurements of mass gains with an accuracy of 5 × 10⁻⁶ g. Temperature fluctuations in the reaction chamber did not exceed ± 1 K and those of liquid sulphur did not exceed ± 0.1 K.

Special design of the spiral suspension (1) allows vertical movements, and by that the introduction of the sample into the reaction chamber when the desired temperature and partial pressure of sulphur vapour had been reached, as well as the interruption of the reaction at any moment by lifting the sample above the reaction space.

The inert gas enters the apparatus through two flowmeters (5, 6). The stream of helium flowing through the upper inlet protects the spiral and makes the condensation of sulphur on the cool parts of the apparatus, impossible. The second gas stream passes through the reservoir with liquid sulphur carrying its vapours to the reaction chamber, where both helium fluxes join together and, after having passed the reaction tube, leave the apparatus, through a liquid-nitrogen sulphur trap (9).

The partial pressure of sulphur vapour in the gas mixtures depends on the flow rates of both helium streams and on the temperature of the liquid sulphur, which creates vast possibilities of obtaining any desired sulphur pressure, ranging between 10⁻¹ and 10⁵ Pa. One of the most important problems in this respect consists in measuring these pressures with sufficient accuracy. There are two such possibilities. The first method, developed by Wakihara *et al.* [16] consists of determining the mass of sulphur condensed in the trap and recalculating it into the sulphur pressure, based on the ideal gas state equation. However, this method cannot be used for determining low sulphur pressures because the amount of sulphur condensed in the trap, even after very long times, is too small to be determined with sufficient accuracy. Thus, a new method of indirect determination of sulphur pressure has been developed, based on an electrical conductivity measurement using an appropriate semiconductive probe, consisting of manganous sulphide doped with vanadium. The electrical conductivity, σ , of this probe as a function of sulphur pressure and temperature is given by

$$\sigma = \sigma_0 p_s^{1/6} \exp \left[- \frac{43.5 \text{ kJ mol}^{-1}}{RT} \right] \quad (1)$$

where σ_0 denotes a constant, which depends on the probe geometry. The absolute values of the conductivity were strictly reproducible, even after several months of working time of the probe (Fig. 4). The constant value of σ , corresponding to the equilibrium

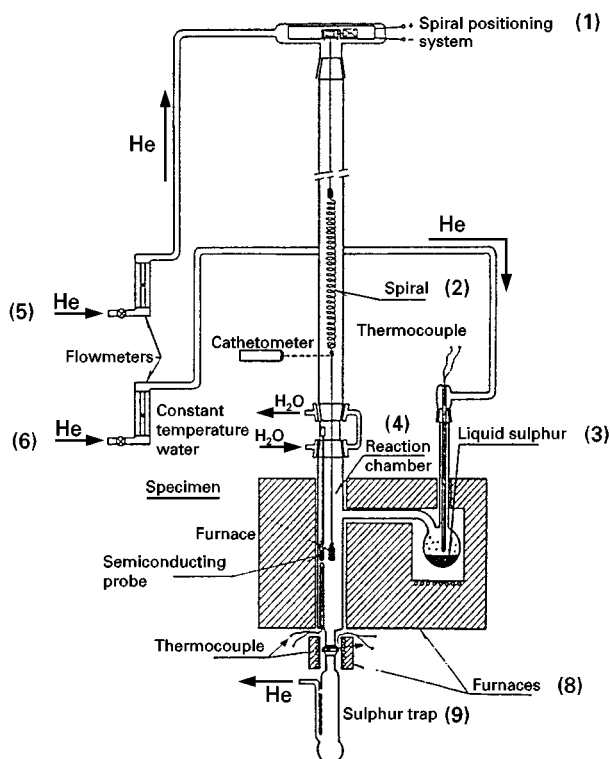


Figure 3 Schematic illustration of the thermogravimetric assembly for studying the kinetics of high-temperature sulphidation of metals.

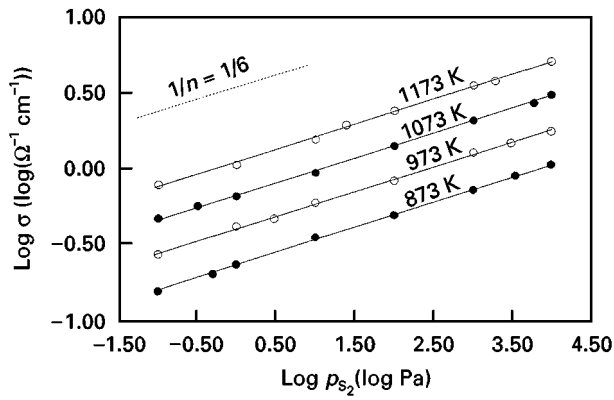


Figure 4 The partial-pressure dependence of the electrical conductivity of vanadium-doped manganous sulphide, for several temperatures ($p_{S_2} < p_{CoS_2}^d$).

conditions, was reached above 900 K after a short time, not exceeding a few minutes. This arrangement thus enabled continuous monitoring of the sulphur pressure in the reaction chamber close to the sulphidized specimen. The details of the preparation and calibration of the discussed semiconducting probe will be described elsewhere [17].

Phase composition of the scales has been studied by various X-ray techniques and their morphology by SEM. The mechanisms of sulphidation were investigated using platinum-wire markers, and also a two-stage sulphidation method [18] with the radiative sulphur ^{35}S isotope as a tracer.

4. Results and discussion

Sulphidation rate measurements revealed that over the whole temperature and sulphur pressure range studied, the sulphidation of cobalt follows, after a certain incubation period, a familiar parabolic law

$$\left(\frac{\Delta m}{A}\right)^2 = k_p t + c \quad (2)$$

where Δm is the weight gain of the sulphidized samples after time t , A is its surface area, k_p the parabolic rate constant of the reaction, and c is a constant.

Figs 5 and 6 show, for illustration, several kinetic runs for different temperatures and sulphur pressures. As can be seen, after a certain incubation period, lasting longer the lower the sulphur pressure, sulphidation of cobalt follows parabolic kinetics, thus being diffusion controlled. The partial-pressure dependence of the sulphidation rate for several temperatures is shown in Fig. 7 as a double logarithmic plot. The dotted lines on this diagram mark the dissociation pressures of CoS_2 and Co_3S_4 phases as a function of temperature. As it can be seen, below the dissociation pressure of CoS_2 the rate of cobalt sulphidation increases gradually with increasing sulphur partial pressure, and above this critical value becomes pressure independent over the entire temperature range studied.

This behaviour of cobalt sulphidation kinetics can satisfactorily be explained in terms of the Co-S phase

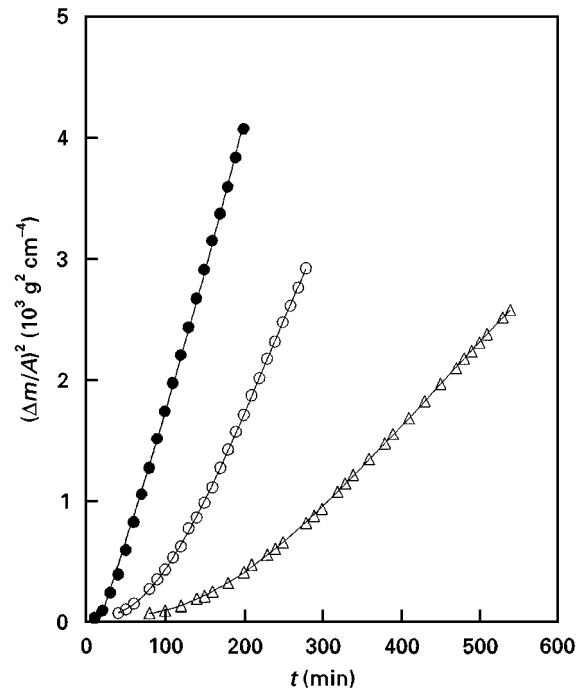


Figure 5 The kinetics of cobalt sulphidation at 923 K for several sulphur pressures. $p_{S_2} < p_{CoS_2}^d$. (Δ) 0.28×10^2 Pa, (\circ) 0.74×10^2 Pa, (\bullet) 1.70×10^2 Pa.

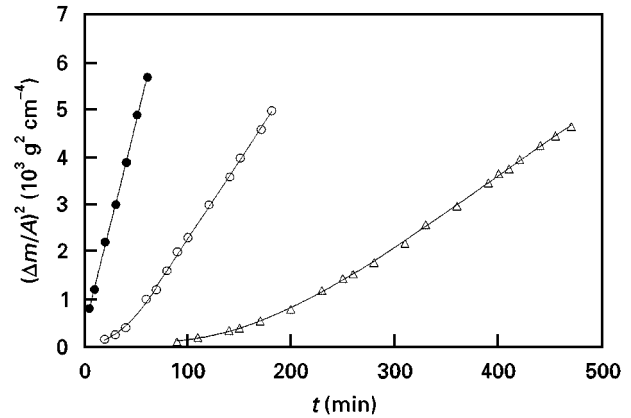


Figure 6 The kinetics of cobalt sulphidation at 1023 K for several sulphur pressures ($p_{S_2} < p_{CoS_2}^d$; p_{S_2} : (Δ) 3.6×10^1 Pa, (\circ) 1.0×10^2 Pa, (\bullet) 2.0×10^3 Pa.

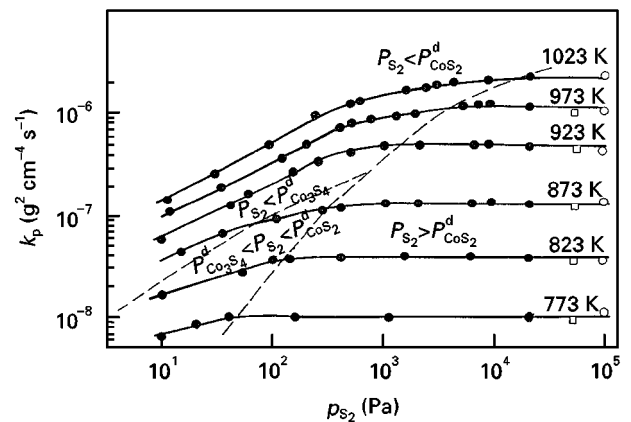


Figure 7 The partial-pressure dependence of the sulphidation rate of cobalt at several temperatures. (\square) [6], (\circ) [10], (\bullet) present work.

diagram, based on the results of phase composition of scales and their morphologies. From the Co-S phase diagram discussed earlier (Fig. 2) it follows that above 900 K the Co_3S_4 is unstable. Thus, at $p_{\text{S}_2} < p_{\text{CoS}_2}^{\text{d}}$ a double layer ($\text{Co}_9\text{S}_8\text{Co}_{1-y}\text{S}$) scale may be expected. X-ray and SEM results confirm these conclusions. From Fig. 8 it follows that under those conditions the scale is double-layered with large columnar crystals of both sulphides typical for the outward lattice diffusion of cations. At higher pressures, on the other hand ($p_{\text{S}_2} > p_{\text{CoS}_2}^{\text{d}}$), a triple-layer scale with a very thin uppermost CoS_2 -layer has been observed (Fig. 9) what is again in agreement with theoretical predictions. This layer is more visible in Fig. 10 because of higher magnification and much longer sulphidation time. In contrast to inner Co_9S_8 and intermediate Co_{1-y}S layers, the outer CoS_2 layer is very fine-grained, as shown in Fig. 11. It is interesting to note that the formation of this layer is preceded by a rather slow nucleation period, as illustrated in Fig. 12. This is probably the reason why other authors [6-9, 15] did not find this compound on the surface of the sulphide scale on cobalt.

At lower temperatures ($T < 900$ K) the phase composition of scales has also been found to agree with theoretical predictions based on the Co-S diagram shown in Fig. 2. At pressures lower than the dissociation pressure of CoS_2 ($p_{\text{S}_2} < p_{\text{CoS}_2}^{\text{d}}$) the scale was triple-layered ($\text{Co}_9\text{S}_8/\text{Co}_{1-y}\text{S}/\text{Co}_3\text{S}_4$) (Fig. 13) and at higher pressure ($p_{\text{S}_2} > p_{\text{CoS}_2}^{\text{d}}$) a four-layered scale has been

found, with an extremely thin uppermost CoS_2 layer, as illustrated in Fig. 14. This micrograph shows only the upper-part fragment of the cross-section of the scale and consequently the fourth, innermost Co_9S_8 layer is not visible.

It has been found that the thickness ratio of the scale sublayers formed at a given p_{S_2} and T was independent of the reaction time as shown in Fig. 15. This strongly suggests that under steady-state conditions (parabolic kinetics) not only the growth rate of the whole scale but also that of each layer is diffusion-controlled, and consequently that local thermodynamic equilibria are established at every phase boundary of the growing scale.

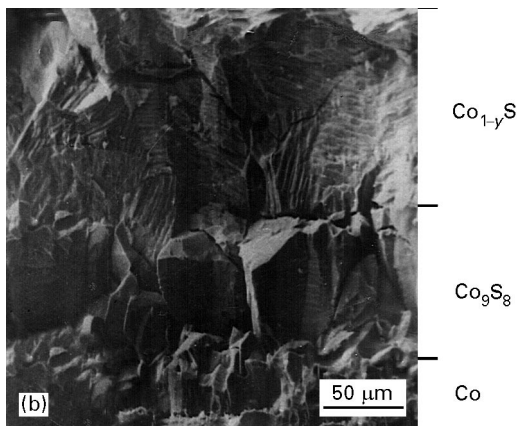
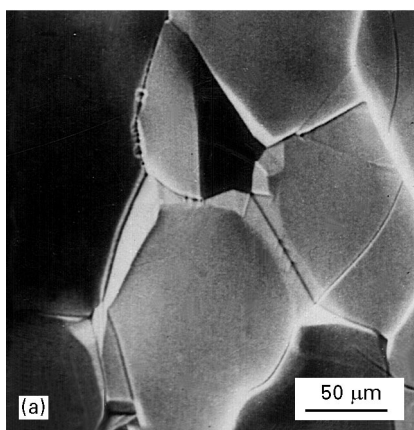


Figure 8 (a) Surface and (b) cross-section of the sulphide scale formed on the cobalt at 973 K and ($p_{\text{S}_2} < p_{\text{CoS}_2}^{\text{d}}$). $p_{\text{S}_2} = 1.5 \times 10^2$ Pa.

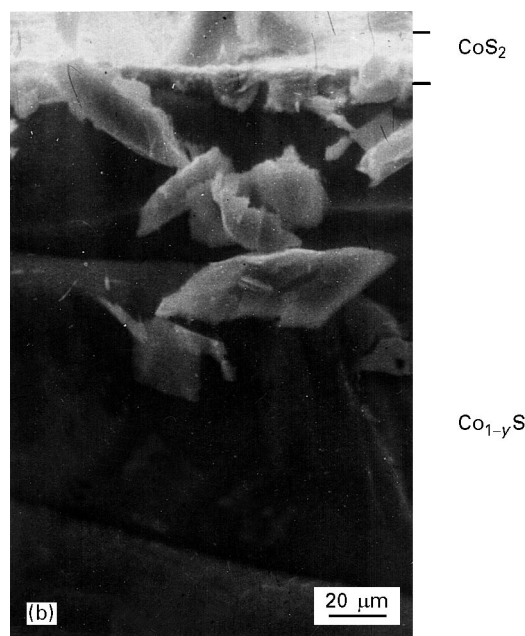
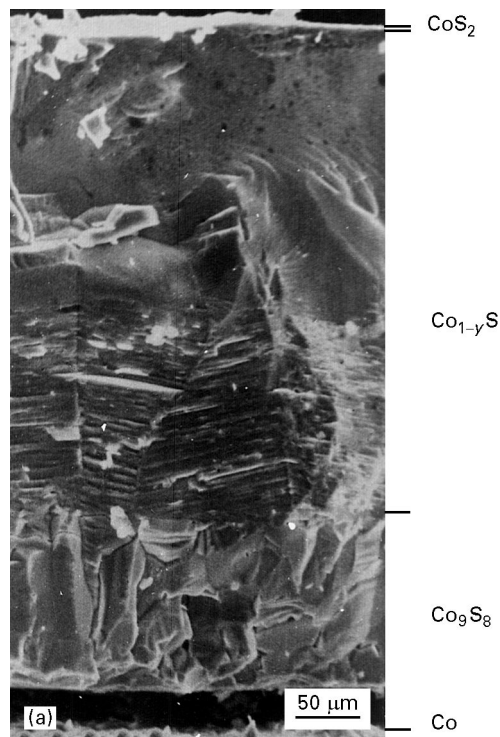


Figure 9 (a, b) Cross-section of the sulphides scale formed on cobalt at 923 K and $p_{\text{S}_2} > p_{\text{CoS}_2}^{\text{d}}$. $p_{\text{S}_2} = 2.0 \times 10^3$ Pa.

It should be noted, however, that the thickness ratio of particular scale layers may change in some cases not only with temperature but also with sulphur pressure. Such a situation has been observed at pressures lower than the dissociation pressure of CoS_2 ($p_{\text{S}_2} < p_{\text{CoS}_2}^{\text{d}}$). Under these conditions the sulphidation rate increases with increasing sulphur pressure (Fig. 7) because the very thin CoS_2 layer cannot be formed on the scale surface. At $T > 900$ K the scale is double-layered (Fig. 8) and the thickness ratio of both scale

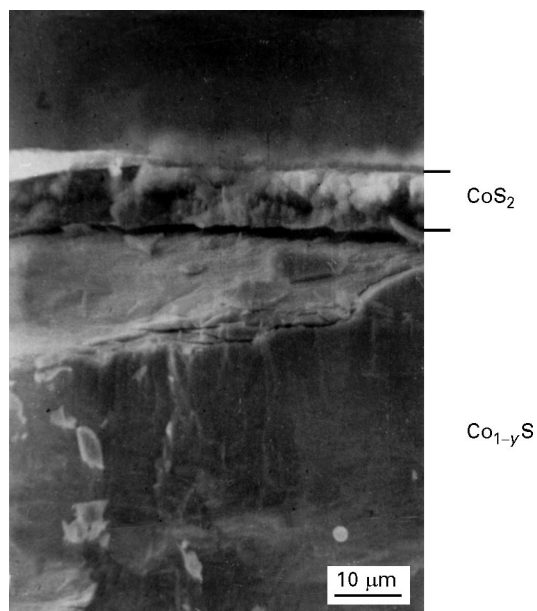


Figure 10 Part of the cross-section of the sulphide scale on cobalt ($T = 923$ K, $p_{\text{S}_2} = 6 \times 10^3$ Pa $> p_{\text{CoS}_2}^{\text{d}}$).

layers increases with increasing sulphur pressure in favour of the outer Co_{1-y}S layer, as illustrated in Fig. 16. The concentration gradient of cation vacancies in this layer, being the driving force for diffusion, increases with sulphur pressure in a way analogous to the non-stoichiometry of cobaltous sulphide (Fig. 17) and consequently the sulphidation rate increase [13, 19]. On the other hand, the concentration gradient of defects in the inner Co_9S_8 layer is not affected by sulphur-pressure changes in the ambient atmosphere, because at the $\text{Co}_9\text{S}_8/\text{Co}_{1-y}\text{S}$ interface sulphur activity is determined by the dissociation pressure of the Co_{1-y}S phases that is constant at a given temperature.

An analogous situation is observed at $T < 900$ K, i.e. when the Co_3S_4 phase is thermodynamically stable. In this case, however, the scale at sulphur pressures lower than the dissociation pressure of CoS_2 is triple-layered ($\text{Co}_9\text{S}_8/\text{Co}_{1-y}\text{S}/\text{Co}_3\text{S}_4$) and the uppermost Co_3S_4 layer constitutes a smaller part of the whole scale than in the previous case (Fig. 13). Consequently, the influence of sulphur pressure on the sulphidation rate of cobalt is weaker than for double-layer scale formation (see Fig. 7).

Based on fragmentary marker experiments, it was assumed in previous papers [7, 9] that the sulphide scale on cobalt grows essentially by the outward diffusion of cations. It has been shown, however, that this method may sometimes lead to incorrect results [18]. Thus, besides systematic marker experiments, a two-stage sulphidation method [20] has been applied in this study, using the radioactive sulphur isotope ^{35}S as a tracer.

Small pieces of platinum wire (diameter $20 \mu\text{m}$) have been scattered on a cobalt sample, which subsequently



Figure 11 Surface of the sulphide scales formed on cobalt at $T > 900$ K and sulphur pressures (a) lower, and (b) higher than the dissociation pressure of CoS_2 .

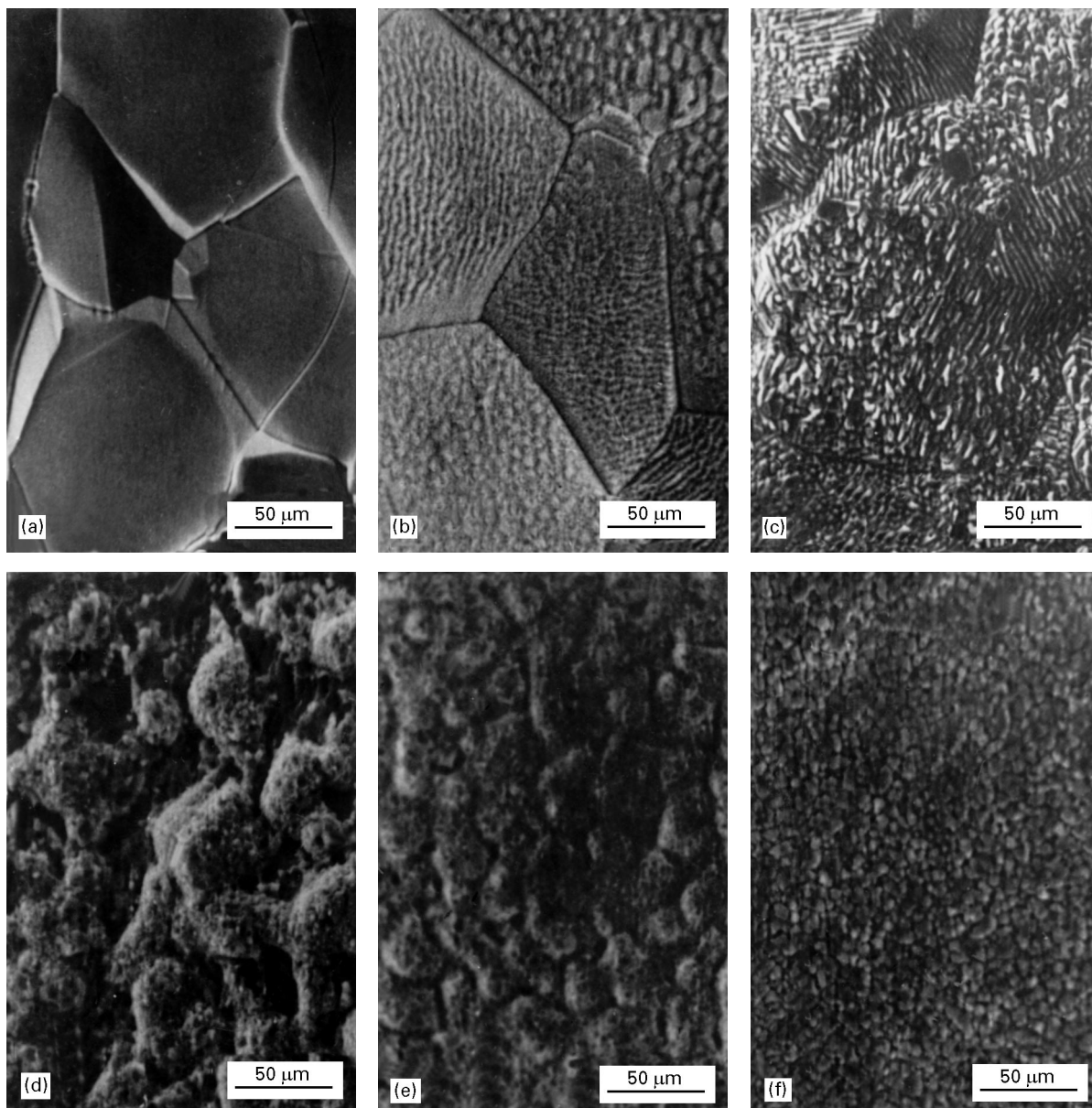


Figure 12 An illustration of the nucleation and growth of the CoS_2 layer on the surface of Co_{1-y}S scale on cobalt at 973 K and $p_{\text{S}_2} > p_{\text{CoS}_2}^d$. (a) 5 min, (b) 10 min, (c) 20 min, (d) 40 min, (e) 80 min, (f) 200 min.

was sulphidized in the horizontal position. After terminating the reaction, the position of the platinum marker in the scale was determined by SEM. It was found that in the entire temperature and pressure range studied, platinum wire markers were located at the metal/scale interface and that this position was independent of the reaction time, and also of the phase composition of the scales. For illustration, a cross-section of a double-layered sulphide scale on cobalt with platinum marker, located at the metal/scale interface, is shown in Fig. 18. These results strongly suggest that, in agreement with previous results [7], the sulphide scale on cobalt grows essentially by the outward diffusion of cations.

To prove this conclusion, two-stage sulphidation experiments have been carried out using the ^{35}S isotope. A metal sample was sulphidized in the first stage in a non-radioactive environment, and then – without braking the reaction – the ^{35}S isotope was introduced

into the reaction chamber and the reaction was continued to obtain approximately a scale which was twice as thick. After terminating the reaction, a perpendicular-to-the core cross-section was made and the distribution of the isotope in the scale was determined autoradiographically. An example of such an autoradiograph is shown in Fig. 19 with a photograph of the scale cross-section. As can be seen, the outer (white) part of the scale, formed during the second stage stage of the reaction, contains the radioactive sulphur isotope, whereas the inner part, formed in the first stage of sulphidation, does not show any evidence of radioactive sulphur. The boundary between the radioactive and non-radioactive part of the scale is sharp and corresponds exactly to the start of the second stage of sulphidation. It can then be inferred that, according to marker results, the sulphide scale on cobalt grows by the outward diffusion of cations. From the autoradiograph shown in Fig. 19 it follows

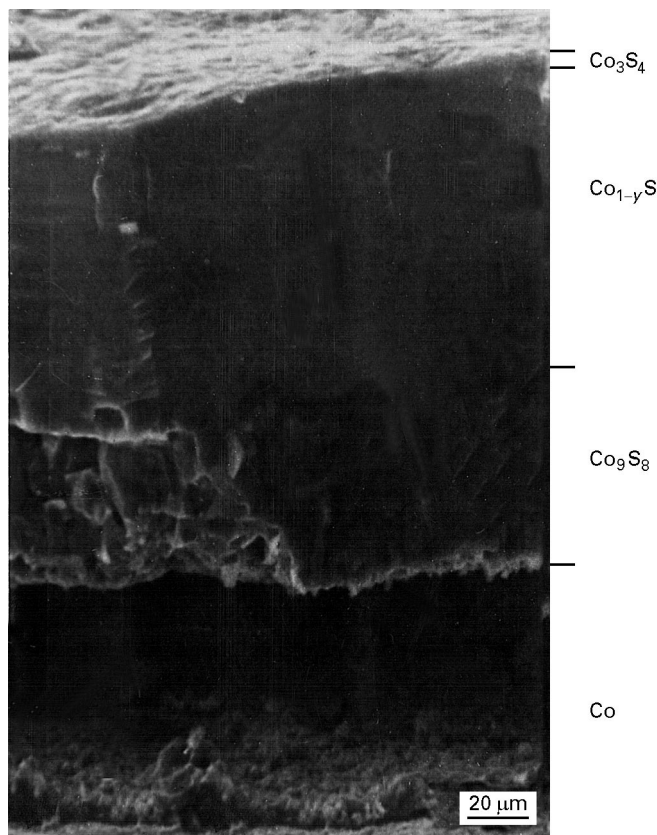


Figure 13 Cross-section of the sulphide scale formed on cobalt at 873 K and $1.5 \times 10^2 \text{ Pa} = p_{\text{S}_2} < p_{\text{CoS}_2}^d \cdot p_{\text{Co}_3\text{S}_4}^d < p_{\text{S}_2} < p_{\text{Co}_9\text{S}_8}^d$.

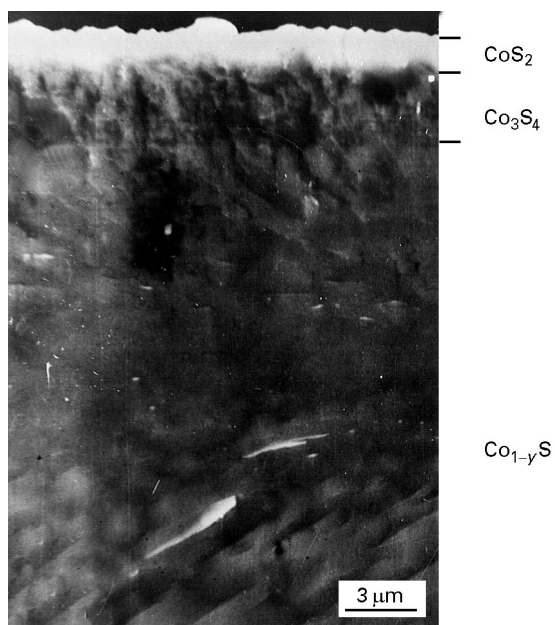


Figure 14 Cross-section of the upper part of the sulphide scale formed on cobalt at 873 K and $6.0 \times 10^3 \text{ Pa} = p_{\text{S}_2} > p_{\text{CoS}_2}^d$.

also that close to the corners of the sulphidized sample, radioactive sulphur penetrated through the initially formed, non-radioactive parts of the scale to the metallic core. It has been shown previously [21, 22] that the inward penetration of the oxidant (sulphur or oxygen) through the scale close to corners of flat specimens results from the formation of dissociation fissures. These fissures are formed in the very

early stages of the reaction owing to the high resistance of plastic deformation of the scale in the vicinity of corners, followed by its dissociation [21–24].

Summarizing these results, it may be concluded that the growth mechanism of the sulphide scale on cobalt by the outward diffusion of cations has been confirmed by both the marker and two-stage sulphidation methods. It is interesting, however, that the results obtained by using radioactive sulphur proved clearly that the compact scale formed on flat areas of the sulphidized sample grows exclusively by the outward diffusion of cations, sulphide ions being practically immobile in cobalt sulphides in comparison with the mobility of cations. Only in the vicinity of corners and curvatures of the metal sample is the participation of inward transport of sulphur possible, due to the formation of the scale of dissociation fissures.

Fig. 20 shows a collective plot of the temperature dependences of the parabolic rate constant for the sulphidation of cobalt determined in the present work on the background of available literature data. It follows from this comparison that at pressures exceeding the dissociation pressure of the CoS_2 phase, there is a fairly good agreement between these and previously obtained kinetic results, concerning both the absolute values of the sulphidation rate and the activation energy of this process. At lower pressures, however, and temperatures exceeding the thermodynamic stability of the Co_3S_4 phase ($T > 900 \text{ K}$), the activation energy of double-layered ($\text{Co}_9\text{S}_8/\text{Co}_{1-y}\text{S}$) scale formation is much smaller ($E_k = 61 \text{ kJ mol}^{-1}$), being less than one-half that for multilayered scale formation ($E_k = 145 \text{ kJ mol}^{-1}$). Finally, under

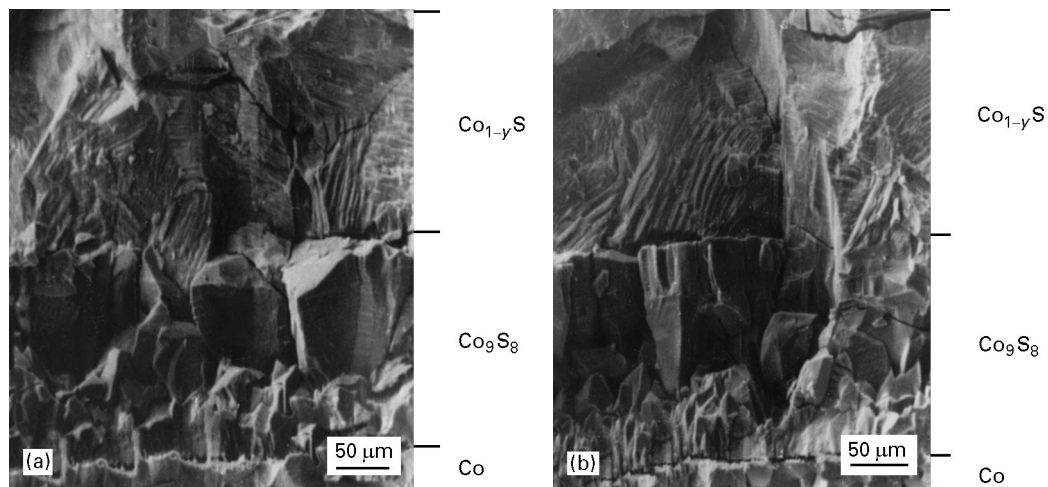


Figure 15 Cross-section of the sulphide scales formed on cobalt for different sulphidation times, at $T > 900$ K and $p_{S_2} < p_{CoS_2}^d$, 1.5×10^2 Pa = (a) $t = 140$ min. (b) $t = 250$ min.

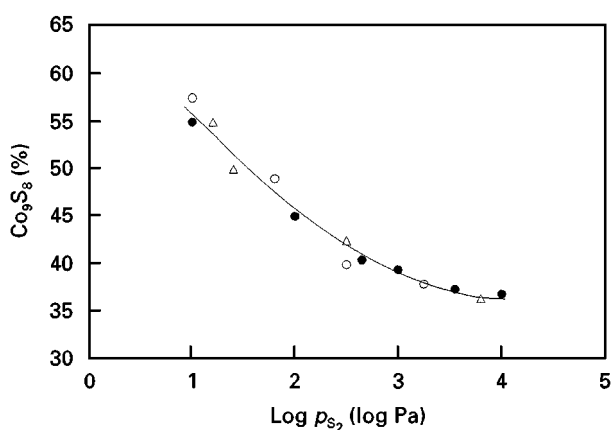


Figure 16 The influence of sulphur pressure on the thickness ratio of $Co_{1-y}S/Co_9S_8$ scale layers growing on cobalt at different temperatures and $p_{S_2} < p_{CoS_2}^d$. (○) 923 K, (●) 973 K, (△) 1023 K.

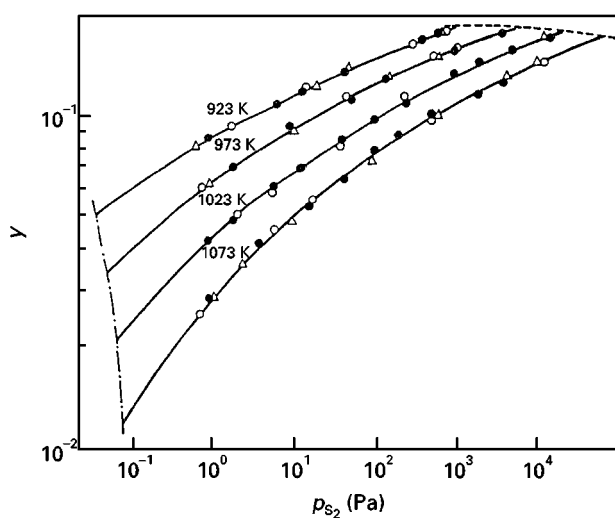


Figure 17 Deviations from stoichiometry of $Co_{1-y}S$ as a function of the sulphur pressure for several temperatures [13, 19]. (—) [13], (●, ○, △) [19], (---) phase boundary of $Co_9S_8/Co_{1-y}S$, (---) phase boundary of $Co_{1-y}S/CoS_2$.

conditions where the Co_3S_4 phase can form ($T < 900$ K), but the CoS_2 phase is still unstable, the activation energy of triple-layered ($Co_9S_8/Co_{1-y}S/Co_3S_4$) scale formation is higher than that for double-

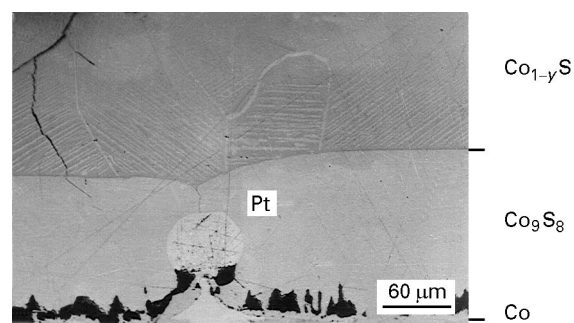


Figure 18 Cross-section of the sulphide scale formed on cobalt at 1023 K and $p_{S_2} = 1 \times 10^3$ Pa. The marker indicates the metal/scale interface.

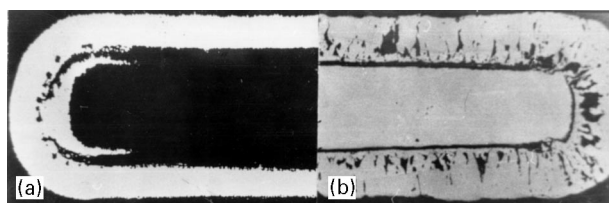


Figure 19 (a) Autoradiogram and (b) photograph of the cross-section of the sulphide scale formed on cobalt in the two-stage sulphidation process, the first stage in natural sulphur, and the second stage in a radiative sulphur environment. $T = 1023$ K, $p_{S_2} = 1.2 \times 10^3$ Pa.

layered ($Co_9S_8/Co_{1-y}S$) scale formation, but still lower than in the case when a CoS_2 layer is formed on the scale surface ($E_k = 130$ kJ mol⁻¹).

This a priori unexpected behaviour becomes understandable if one considers the fact that the increase of the rate of multilayer scale formation results not only from increasing temperature but also from increasing the sulphur partial pressure at the $Co_{1-y}S/CoS_2$ or Co_3S_4/CoS_2 interface. Consequently, the apparent activation energy of sulphidation at pressures lower than the dissociation pressure of the CoS_2 phase is lower than that of multilayer scale formation, as illustrated in Fig. 21. It is interesting that slope changes of

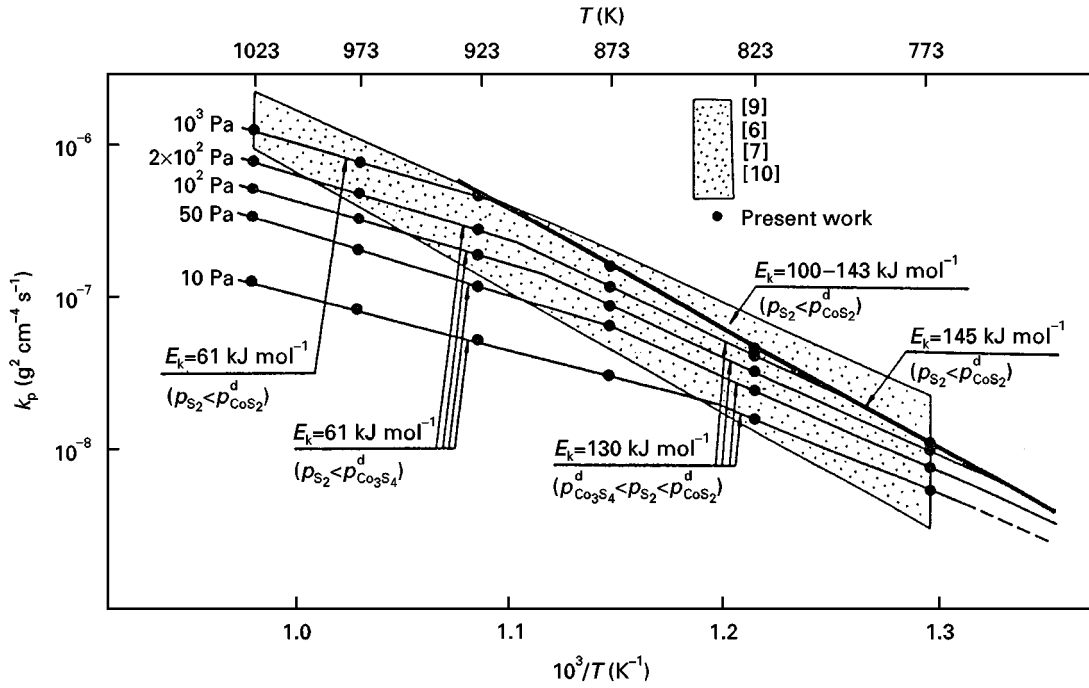


Figure 20 Temperature dependence of the sulphidation rate of cobalt for several sulphur pressures, on the background of available literature data [6–10].

Arrhenius plots in Fig. 21 correspond very well with dissociation pressures of CoS_2 or Co_3S_4 sulphides. With respect to this, it should be noted that the activation energy, E_k , of multilayer scale formation is purely apparent and has no physical meaning, because it reflects not only the effect of temperature but also that of sulphur pressure on the sulphidation kinetics. However, at pressures lower than the dissociation pressure of CoS_2 or Co_3S_4 the activation energy of sulphidation can also be unrelated to the activation energy of cation diffusion in the scale, because it is still heterogeneous ($\text{Co}_9\text{S}_8/\text{Co}_{1-y}\text{S}$), both sulphides participating in comparable amounts in the scale formation.

Further information is necessary concerning the growth rates of particular scale layers to obtain a better insight into the mechanisms of cobalt sulphidation. At present, the dependence of the sulphidation rate on temperatures and sulphur pressure can roughly be described by the following empirical formula

$$k_p = \text{const } p_{\text{S}_2}^{1/n} \exp\left(-\frac{E_k}{RT}\right) \quad (3)$$

where the exponent $1/n$ varies from $1/2$ to $1/4$ for pressures lower than the dissociation pressure of CoS_2 phase and equals zero for higher pressures. The apparent activation energy, E_k , in turn, changes from 60 kJ mol^{-1} to 145 kJ mol^{-1} when passing from double- to multilayer scale.

Kinetic results clearly suggest that the rate of cobalt sulphidation is very high, even at moderate temperatures. In fact, these rates are more than three orders of magnitude higher than those of cobalt oxidation in the same temperature range [26], as illustrated in Fig. 22. The question then arises whether the very poor protective properties of the sulphide scale on cobalt result from high point-defect concentration,

and thereby very fast volume diffusion of cations, or if the grain-boundary diffusion plays an important role.

To discuss this important question, one has to know the transport properties of all the cobalt sulphides participating in the scale formation, and in particular those of Co_9S_8 and Co_{1-y}S . As already mentioned, no information is available concerning defect structure and self-diffusion in Co_9S_8 , but defect equilibria and chemical diffusion in non-stoichiometric cobaltous sulphide (Co_{1-y}S) have been studied in detail [19]. Using these data one can calculate the growth rate of Co_{1-y}S layer as a function of temperature and sulphur activity by volume diffusion and compare the results of these calculations with experimentally determined values.

The chemical diffusion coefficient in Co_{1-y}S has been found to be independent of sulphide composition (deviation from stoichiometry y) and can be described as a function of temperature by the following empirical equation [24]

$$\tilde{D}_{\text{CoS}} = 0.29 \exp\left(-\frac{110 \pm 8.4 \text{ kJ mol}^{-1}}{RT}\right) \text{ cm}^2 \text{ s}^{-1} \quad (4)$$

From Wagner's theory of metal oxidation [25] it follows that, in the case under discussion, the rate of Co_{1-y}S layer formation is related to \tilde{D}_{CoS} by the following simple equation

$$k'_p = \tilde{D}_{\text{CoS}} (X_V^{(a)} - X_V^{(i)}) \quad (5)$$

where k'_p is the parabolic rate constant of Co_{1-y}S formation, expressed in $\text{cm}^2 \text{ s}^{-1}$, $X_V^{(a)}$ and $X_V^{(i)}$ denote cation vacancy concentrations, expressed in mole fractions, at the outer and inner phase boundaries of the growing Co_{1-y}S layer, i.e. at $T > 900 \text{ K}$ and $p_{\text{S}_2} < p_{\text{CoS}_2}^d$ at $\text{Co}_{1-y}\text{S}/\text{S}_2$ and $\text{Co}_9\text{S}_8/\text{Co}_{1-y}\text{S}$ interface,

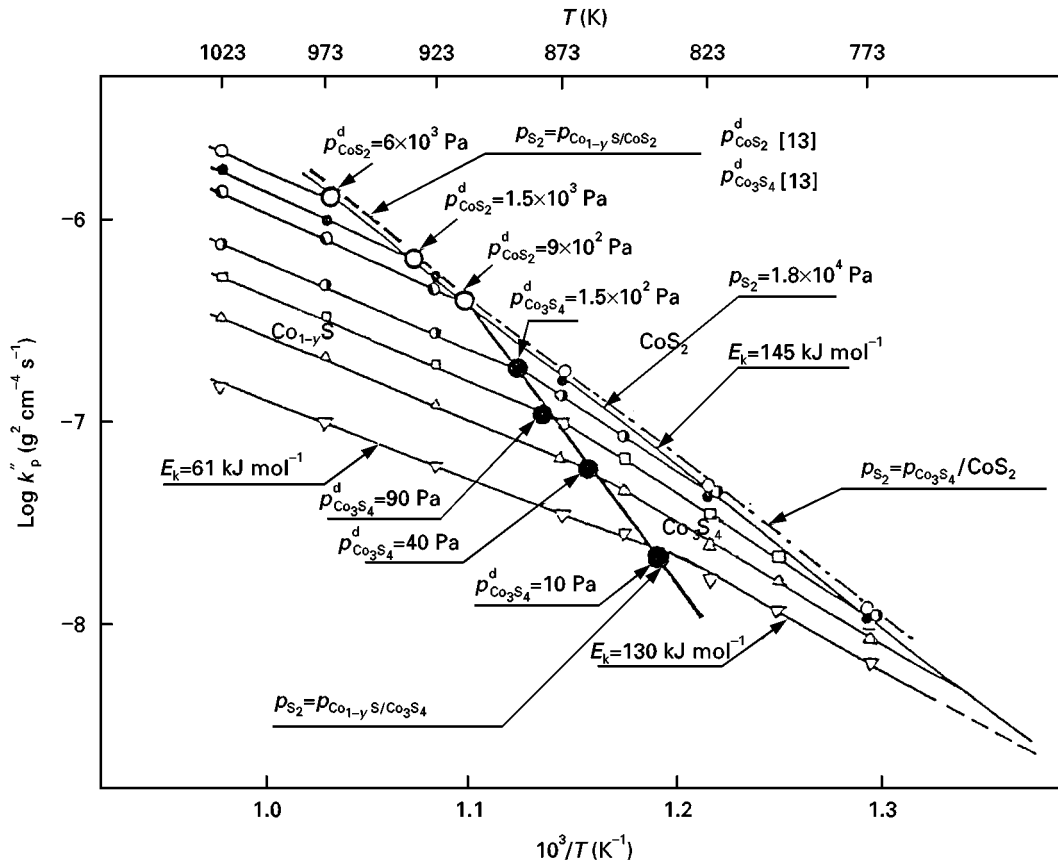


Figure 21 Temperature dependence of the sulphidation rate of cobalt for several sulphur pressures; (○) dissociation pressures of CoS_2 , (●) dissociation pressure of Co_3S_4 . p_{S_2} : (○) 8×10^3 Pa, (●) 2×10^3 Pa, (◐) 10^3 Pa, (◑) 2×10^2 Pa, (□) 10^2 Pa, (△) 50 Pa, (▽) 10 Pa.

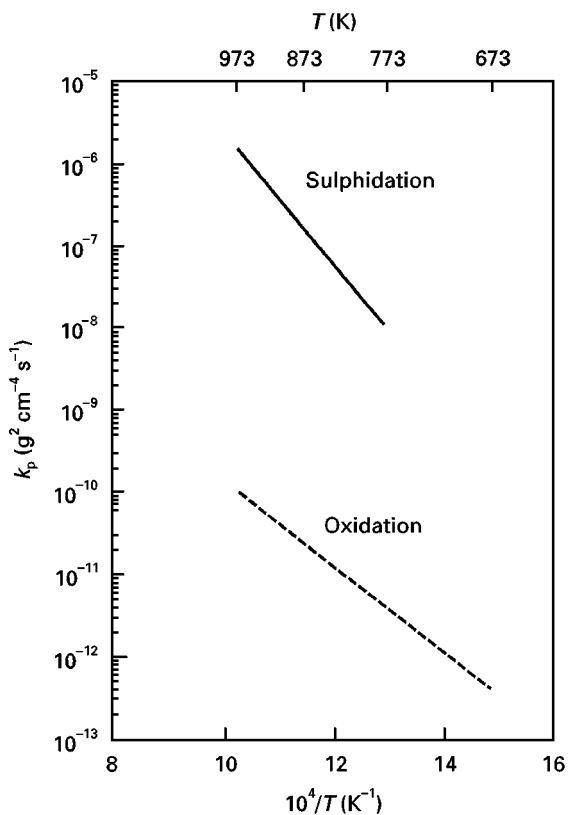


Figure 22 The parabolic rate constants for the sulphidation and oxidation of cobalt as a function of temperature [26].

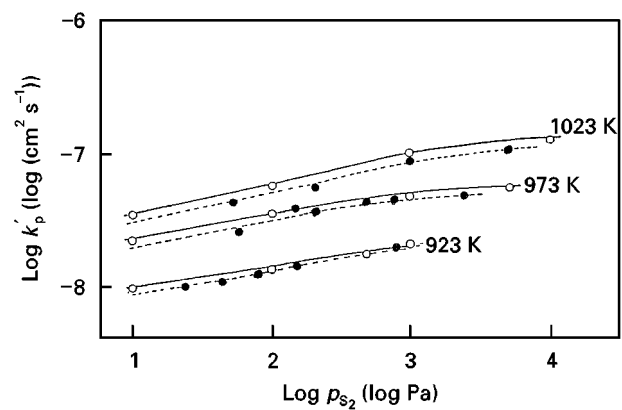


Figure 23 The pressure dependence of the growth rate of the Co_{1-y}S scale on cobalt at several temperatures: (●) experimentally determined from the sulphidation kinetics, (○) calculated from \bar{D}_{CoS} and non-stoichiometry, y .

respectively. This vacancy concentration is equal to the non-stoichiometry of the growing Co_{1-y}S layer. Consequently

$$(X_{\text{V}}^{(a)'} - X_{\text{V}}^{(i)'}) = (y^{(a)} - y^{(i)}) = \Delta y \quad (6)$$

where y is the deviation from stoichiometry of Co_{1-y}S . Equation (5) may then be written in the following form

$$k_p' = \bar{D}_{\text{CoS}} \Delta y \quad (7)$$

Δy values can be calculated from the known deviation from stoichiometry of the Co_{1-y}S [13, 19]. Using these data and Equation 4, k'_p has been calculated as a function of temperature and sulphur activity for the T and p_{S_2} range where the double-layer ($\text{Co}_9\text{S}_8/\text{Co}_{1-y}\text{S}$) scale is formed. The results of these calculations are shown in Fig. 23. on the background of experimentally determined rates of Co_{1-y}S formation. The latter values of k'_p have been obtained from measurements of the thickness of the Co_{1-y}S layer as a function of sulphidation time.

As can be seen, the agreement between calculated and experimentally determined growth rates of the Co_{1-y}S layer is satisfactory, clearly suggesting that the rate-determining step is the *volume* diffusion of cations. Making analogous calculations for Co_9S_8 and Co_3S_4 layers, is impossible, because defect and transport properties of these sulphides are unknown. However, analogous to Co_{1-y}S , the morphology of Co_9S_8 and Co_3S_4 sulphide layers, characterized by large columnar crystals, is typical for the outward volume diffusion of cations. This observation strongly suggests that the whole, heterogeneous, multilayer sulphide scale of cobalt grows by the volume diffusion of cations.

5. Conclusions

The results described in the present paper allow the following conclusions to be formulated.

1. The sulphidation of cobalt at elevated temperatures (773–1073 K) and sulphur pressures ($10\text{--}10^5$ Pa) is diffusion controlled, the rate-determining step being the outward *volume* diffusion of cations.

2. The rate of sulphide corrosion of cobalt is comparable with that of iron and nickel, being about four orders of magnitude higher than the oxidation rate of this metal.

3. Rapid degradation of cobalt in a sulphur atmosphere results mainly from a very high defect concentration in Co_{1-y}S and Co_9S_8 sulphides, participating in comparable amounts in the scale formation on this metal at $T > 900$ K. The only sulphide of cobalt in which the defect concentration seems to be very low is CoS_2 , the growth rate of this sulphide layer being more than two orders of magnitude lower than that of other cobalt sulphides.

4. According to the phase diagram of the cobalt–sulphur system, the sulphide scale on cobalt is heterogeneous. At pressure higher than the dissociation pressure of CoS_2 and temperatures exceeding thermodynamic stability of the Co_3S_4 phase ($T > 900$ K) the scale is triple layered ($\text{Co}_9\text{S}_8/\text{Co}_{1-y}\text{S}/\text{CoS}_2$) and its growth rate shows a negligible dependence on the sulphur partial pressure. At lower partial pressures, the rate of double-layered ($\text{Co}_9\text{S}_8/\text{Co}_{1-y}\text{S}$) scale formation increases with increasing sulphur partial pressure in an analogous way to the concentration of cation vacancies in Co_{1-y}S , according to the classical Wagner model.

5. At lower temperatures ($T < 900$ K), the scale may be four layered ($\text{Co}_9\text{S}_8/\text{Co}_{1-y}\text{S}/\text{Co}_3\text{S}_4/\text{CoS}_2$), triple-layered ($\text{Co}_9\text{S}_8/\text{Co}_{1-y}\text{S}/\text{Co}_3\text{S}_4$), or double-layered ($\text{Co}_9\text{S}_8/\text{Co}_{1-y}\text{S}$), depending on the partial

pressure of sulphur in the ambient atmosphere. Under these conditions again the multilayer scale formation, with the uppermost CoS_2 layer, is independent of sulphur partial pressure.

6. The apparent activation energy of sulphidation is considerably higher for multilayer scales with the uppermost CoS_2 layer, than that for double-layered ($\text{Co}_9\text{S}_8/\text{Co}_{1-y}\text{S}$) scales because the main part of the multilayer scales is growing at the dissociation pressure of CoS_2 that increases with increasing temperature.

Acknowledgements

The present paper was sponsored by the Ministry of Education and the Polish State Committee for Scientific Research under contract AGH No. 11.160.169 during 1993.

References

1. M. F. ROTHMAN, "High Temperature Corrosion in Energy Systems" (Metallurgical Society of AIME, New York, 1995).
2. P. KOFSTAD, "High Temperature Corrosion" (Elsevier Applied Science, London, New York, 1988) p. 425.
3. S. MROWEC and K. PRZYBYLSKI, *High Temp. Mater. Process.* **6** (1984) 1.
4. *Idem.*, *Oxid. Metals* **23** (1985) 107.
5. D. B. MEADOWCROFT and M. J. MANNING, "Corrosion-Resistant Materials for Coal Gasification Systems" (Elsevier Applied Science, London, 1983).
6. A. DEVIN, *Cobalt* **30** (1966) 19.
7. D. COUTSOURADIS and A. DEVIN, in "High Temperature Metallic Corrosion by Sulphur and Its Compounds", edited by Z. A. Foroulis (Corrosion Division of the Electrochemical Society Inc., New York, 1970) p. 132.
8. D. P. WHITTLE, S. VERMA and J. STRINGER, *Corros. Sci.* **13** (1973) 247.
9. S. MROWEC, and T. WERBER, *Fiz. Metallov Metallovid.* **14** (1962) 770.
10. T. BIEGUN, A. BRÜCKMAN and S. MROWEC, *Oxid. Metals.* **12** (1978) 157.
11. T. ROSENQUIST, *J. Iron Steel Inst.* **176** (1954) 37.
12. T. LEEGAARD and T. ROSENQUIST, *Z. Anorg. Allg. Chem.* **328** (1964) 294.
13. H. RAU, *J. Phys. Chem. Solids* **37** (1976) 931.
14. Y. O. CHEN and Y. A. CHANG, *Metall. Trans.* **9B** (1978) 61.
15. I. BARTKOWICZ and A. STOKŁOSA, *Solid State Ionics* **23** (1987) 51.
16. M. WAKIHARA, T. UHIDA and T. TANIGUCHI, *Mater. Res. Bull.* **11** (1976) 973.
17. A. WÓJTOWICZ, Phd Thesis, University of Mining and Metallurgy, Cracow, 1989.
18. E. W. A. YOUNG and J. M. W. de WIT, *ibid.* **14** (1985) 39.
19. M. DANIELEWSKI, S. MROWEC and A. WÓJTOWICZ, *Oxid. Metals.* **35** (1991) 223.
20. S. MROWEC and T. WERBER, *Werstoffe Korrosion* **19** (1968) 944.
21. S. MROWEC, *Corros. Sci.* **7** (1967) 563.
22. A. BRÜCKMAN, *ibid.* **7** (1967) 51.
23. A. BRÜCKMAN and J. ROMAŃSKI, *ibid.* **5** (1965) 185.
24. S. MROWEC, in "High Temperature Corrosion" Proceedings of JIMIS-3, (Transactions of the Japan Institute of Metals, Tokyo, 1983) p. 69.
25. P. KOFSTAD, "High Temperature Corrosion" (Elsevier Applied Science, London, New York, 1988) p. 163.
26. J. PAIDASSI, M. VALLEE and P. PEPIN, *Mem. Sci. Rev. Metall.* **62** (1965) 789.

Received 18 February
and accepted 5 December 1997